Electric-Field Gradient Tensor in Ferrous Compounds*

R. INGALLS†
Carnegie Institute of Technology, Pittsburgh, Pennsylvania
(Received 1 August 1963)

The electric-field gradient tensor at the iron nucleus in ferrous (Fe^{2+}) compounds is investigated. One sees that under the combined action of axial and rhombic crystalline fields and the spin-orbit interaction, the ferrous-ion ($^5D,3d^6$)d_ϵ states produce a large, temperature-dependent, contribution to the electric-field gradient tensor. It is found that this direct contribution is diminished by that from the lattice itself (the second-order axial and rhombic components of the crystalline field), as well as Sternheimer polarization effects and covalency. The results of this investigation are then applied to Mössbauer results in $FeSiF_6\cdot 6H_2O$ to obtain an estimate of the electric quadrupole moment of Fe^{57m} (0.29 ± 0.02b), which is in agreement with that from ferric (Fe^{3+}) studies. Finally, estimates also based upon Mössbauer measurements, are made of the d_ϵ energy splittings in the ferrous compounds, $FeSiF_6\cdot 6H_2O$, $FeSO_4\cdot 7H_2O$, $FeC_2O_4\cdot 2H_2O$, $Fe(NH_4SO_4)_2\cdot 6H_2O$, $FeSO_4$, $FeCl_2\cdot 4H_2O$, and FeF_2.

I. INTRODUCTION

IN Mössbauer experiments, with ferrous (Fe^{2+}) compounds,[1–5] values were found for the Fe^{57m} electric quadrupole splitting ΔE which, in general, are temperature-dependent and vary from compound to compound (Fig. 1). The pertinent interaction, expressed in terms of Q, the quadrupole moment of Fe^{57m}, the nuclear spin operator, $\mathbf{I}$, and the components of the electric-field gradient (EFG) tensor at the position of the nucleus, V_{xx}, V_{yy}, and V_{zz}, is as follows[6]:

$$\mathcal{H}=\frac{eQ}{4I(2I-1)}\{V_{zz}[3I_z^2-I(I+1)]+(V_{xx}-V_{yy})(I_x^2-I_y^2)\}. \quad (1)$$

For Fe^{57m} with spin $\frac{3}{2}$, the resulting quadrupole splitting is

$$\Delta E=\tfrac{1}{2}e^2qQ[1+\tfrac{1}{3}\eta^2]^{1/2}, \quad (2)$$

where the above EFG components are conveniently expressed[6,7]:

$$V_{zz}/e=q=(1-R)q_{\rm val}+(1-\gamma_\infty)q_{\rm lat} \quad (3)$$

and correspondingly

$$(V_{xx}-V_{yy})/e=\eta q=(1-R)\eta_{\rm val}q_{\rm val}+(1-\gamma_\infty)\eta_{\rm lat}q_{\rm lat}. \quad (4)$$

In these expressions the subscript "val" refers to the charge distribution of the aspherical $3d$-"valence" electron belonging to the ferrous ion ($^5D,3d^6$). The subscript "lat" refers to the charge distribution of the neighboring ions in the crystalline lattice. The Sternheimer factors,[7–8] $(1-R)$ and $(1-\gamma_\infty)$, are added to correct for the polarization of the ferric-like ($^6S,3d^5$) core by the EFG of the valence and lattice charge distributions.

The most important contribution to q, in Eq. (3) is $q_{\rm val}$, which has an absolute value of[9] $(4/7)\langle 1/r^3\rangle_{3d}$ for the free ion, neglecting the spin-orbit interaction. However, this term, itself, is reduced from the free-ion value by the crystalline field at finite temperatures (Sec. II), the spin-orbit interaction (Sec. III), and covalency effects (Sec. V). In addition, the factors, $(1-R)$, and $(1-\gamma_\infty)q_{\rm lat}$ (Sec. IV), further reduce the effect of this term. These arguments also hold for the quantity, $\eta_{\rm val}q_{\rm val}$, in Eq. (4), which is present when the valence charge distribution is not symmetric about the z axis. Thus, when all the contributions to the EFG are simultaneously treated, one obtains a significantly larger value for the quadrupole moment, Q, than if one were to use the free-ion approximation (Sec. VI). At the same time it is also possible to make reasonable estimates of the crystal-field splittings in several compounds (Sec. VII) based upon the Mössbauer data of Fig. 1.

II. PRIMARY EFFECT OF THE CRYSTALLINE FIELD

The primary effect of the crystalline field is to lift the fivefold spatial degeneracy of the ^5D state of the free-ferrous ion, splitting it into a series of orbital states, ψ_n, of energies, ϵ_n, which may each produce different EFG tensors at the position of the nucleus. (Each of these orbital states will still have fivefold spin degeneracy.) Assuming the thermal transition times between

* Supported by the Office of Naval Research and the National Science Foundation.

† Present address: Physics Department, University of Illinois, Urbana, Illinois.

[1] G. K. Wertheim, Phys. Rev. **121**, 63 (1961).

[2] S. DeBenedetti, G. Lang, and R. Ingalls, Phys. Rev. Letters **6**, 60 (1961).

[3] W. Kerler, Z. Physik **167**, 194 (1962).

[4] C. E. Johnson, W. Marshall, and G. J. Perlow, Phys. Rev. **126**, 1503 (1962).

[5] R. Ingalls, Ph.D. thesis, Department of Physics, Carnegie Institute of Technology, Pittsburgh, Pennsylvania, May, 1962 (unpublished).

[6] M. H. Cohen and F. Reif, *Solid State Physics*, edited by F. Seitz and D. Turnbull (Academic Press Inc., New York, 1957), Vol. 5.

[7] R. Ingalls, Phys. Rev. **128**, 1155 (1962). H. M. Foley, R. M. Sternheimer, and D. Tycko, Phys. Rev. **93**, 734 (1954); R. M. Sternheimer and H. M. Foley, *ibid.* **102**, 731 (1956); R. M. Sternheimer, *ibid.* **84**, 244 (1951); **95**, 736 (1954); **105**, 158 (1957).

[8] A. J. Freeman and R. E. Watson, Phys. Rev. **131**, 2566 (1963).

[9] A. Abragam and F. Boutron, Compt. Rend. **252**, 2404 (1961).

TABLE I. Expectation values of several operators used in calculating axial and rhombic crystalline-field splittings, and EFG components, for the orbital states of the ferrous ion.

Orbital wave functions ψ_n	$\langle 3L_z^2-L(L+1)\rangle_n$	$\langle V_{\text{axial}}\rangle_n$	$\langle V_{zz}/e\rangle_n$	$\langle 3L_x^2-3L_y^2\rangle_n$	$\langle V_{\text{rhomhic}}\rangle_n$	$\langle (V_{xx}-V_{yy})/e\rangle_n$
$\lvert 3z^2-r^2\rangle$	-6	$(4/7)B_2^0\langle r^2\rangle$	$-(4/7)\langle r^{-3}\rangle$	0	0	0
$\lvert x^2-y^2\rangle$	6	$-(4/7)B_2^0\langle r^2\rangle$	$(4/7)\langle r^{-3}\rangle$	0	0	0
$\lvert xz\rangle$	-3	$(2/7)B_2^0\langle r^2\rangle$	$-(2/7)\langle r^{-3}\rangle$	-9	$(6/7)B_2^2\langle r^2\rangle$	$-(6/7)\langle r^{-3}\rangle$
$\lvert yz\rangle$	-3	$(2/7)B_2^0\langle r^2\rangle$	$-(2/7)\langle r^{-3}\rangle$	9	$-(6/7)B_2^2\langle r^2\rangle$	$(6/7)\langle r^{-3}\rangle$
$\lvert xy\rangle$	6	$-(4/7)B_2^0\langle r^2\rangle$	$(4/7)\langle r^{-3}\rangle$	0	0	0

these levels[10,11] ($10^{-9}-10^{-11}$ sec) are much shorter than the quadrupole precession times ($\sim 10^{-8}$ sec), the quantities q_{val} and $\eta_{\text{val}}q_{\text{val}}$, become the following ensemble averages[5,12–14]:

$$q_{\text{val}}=Z^{-1}\sum_n \langle V_{zz}/e\rangle_n e^{-\epsilon_n/kT} \tag{5}$$

$$\eta_{\text{val}}q_{\text{val}}=Z^{-1}\sum_n \langle (V_{xx}-V_{yy})/e\rangle_n e^{-\epsilon_n/kT}, \tag{6}$$

where

$$\langle V_{zz}/e\rangle_n=-\langle (3z^2-r^2)/r^5\rangle_n,$$
$$\langle (V_{xx}-V_{yy})/e\rangle_n=-\langle 3(x^2-y^2)/r^5\rangle_n$$

and

$$Z=\sum_n e^{-\epsilon_n/kT}.$$

To determine the wave functions and energies for these calculations, one first operates upon the ^5D state with the crystalline-field perturbation appropriate to a distorted octahedron of surrounding negative ions[15]:

$$V=V_{\text{cubic}}+V_{\text{axial}}+V_{\text{rhombic}} \tag{7}$$
$$=C_4(x^4+y^4+z^4-\tfrac{3}{5}r^4)+B_2^0(3z^2-r^2)+3B_2^2(x^2-y^2).$$

In this expression we have chosen the crystalline-field axes to pass through the neighboring ions. Therefore, V_{axial} corresponds to tetragonal symmetry. However, the features of the EFG tensor are almost unchanged in the case of trigonal symmetry, where the z axis is along the (1,1,1) direction of the octahedron. In either case, C_4 is positive. It should also be mentioned that the smaller, but finite, fourth-order axial ($\sim 35z^4-30z^2r^2+3r^4$), and rhombic [$\sim r^2(x^2-y^2)$] terms have been neglected.

The effects of the crystalline field in Eq. (7) are illustrated in Fig. 2. Operator techniques[15] may be used to show that the cubic term (C_4) splits the ^5D state by an amount, $(4/21)C_4\langle r^4\rangle$, into two groups, the higher, d_γ, composed of orbital states transforming like $3z^2-r^2$ and x^2-y^2; the lower, d_ϵ, composed of orbital states transforming like xz, yz, and xy. The axial (B_2^0) and rhombic (B_2^2) fields further split these groups. It is useful to calculate these splittings by the operator method here, since at the same time, we will obtain the expressions needed for the expectation values in Eqs. (5) and (6). The relevant relationship is[15]

$$\langle L,M_L\ f(r)\left|\begin{Bmatrix} 3z^2-r^2 \\ 3x^2-3y^2\end{Bmatrix}\right|L,M_L\rangle$$
$$=C_L\langle L,M_L\left|\begin{Bmatrix} 3L_z^2-L(L+1) \\ 3L_x^2-3L_y^2\end{Bmatrix}\right|L,M_L\rangle \tag{8}$$

where, for $L=2$,

$$C_L=\frac{\langle L,L|f(r)(3z^2-r^2)|L,L\rangle}{L(2L-1)}$$
$$=-\frac{(4/7)\langle r^2f(r)\rangle}{6}=-\frac{2}{21}\langle r^2f(r)\rangle \tag{9}$$

so that

$$V_{\text{axial}}=-(2/21)B_2^0\langle r^2\rangle[3L_z^2-L(L+1)]$$
$$V_{\text{rhombic}}=-(2/21)B_2^2\langle r^2\rangle[3L_x^2-3L_y^2]. \tag{10}$$

With the use of these expressions, Table I is formed. From it one observes that the axial field separates $|xz\rangle$ and $|yz\rangle$ from $|xy\rangle$ by an amount $(6/7)B_2^0\langle r^2\rangle$. Similarly,

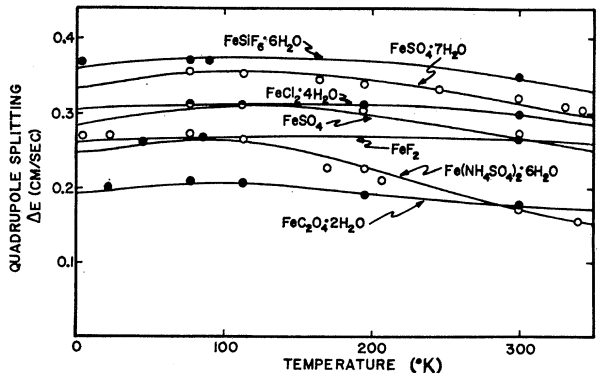

FIG. 1. Experimental quadrupole splittings in ferrous compounds as determined by Mössbauer measurements. The solid lines represent calculations reported in this work. Sources for the experimental data are: $FeSiF_6\cdot 6H_2O$, Ref. 4; $FeSO_4\cdot 7H_2O$, Refs. 3 and 12; $FeCl_2\cdot 4H_2O$, Ref. 12; $FeSO_4$, Ref. 5; FeF_2, Ref. 1; $Fe(NH_4SO_4)_2\cdot 6H_2O$, Refs. 3, 12, and P. Zory (private communication); $FeC_2O_4\cdot 2H_2O$, Ref. 5 and P. Zory (private communication).

[10] M. Tinkham, Proc. Roy. Soc. (London) **A236**, 535 (1956).
[11] T. Ohtsuka, H. Abe, and E. Kanda, Sci. Rept. Tohoku Univ. **9A**, 476 (1957).
[12] L. G. Lang, S. DeBenedetti, and R. Ingalls, J. Phys. Soc. Japan, **17**, Suppl. B-1, 131 (1962).
[13] R. Bauminger, S. G. Cohen, A. Marinov, and S. Ofer, Phys. Rev. Letters **6**, 467 (1961).
[14] H. Eicher, Z. Physik **171**, 582 (1963).
[15] B. Bleaney and K. W. H. Stevens, Repts. Progr. Phys. **16**, 108 (1953).

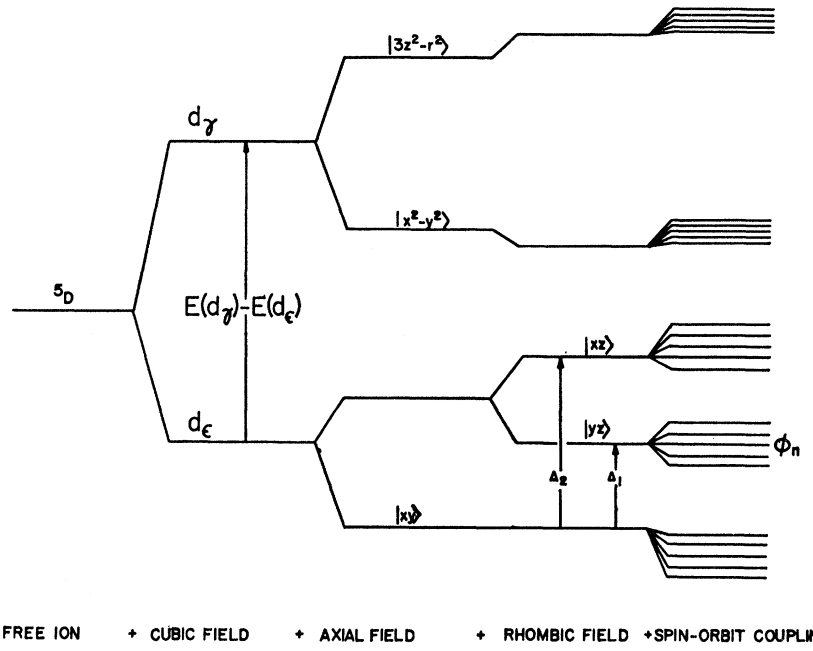

FIG. 2. Energy level scheme for the ferrous ion under the action of the crystalline field plus spin-orbit coupling.

the rhombic field separates $|xz\rangle$ from $|yz\rangle$ by an amount $(12/7)B_2^2\langle r^2\rangle$. Therefore, neglecting fourth-order axial and rhombic terms, the net displacements of $|yz\rangle$ and $|xz\rangle$ from $|xy\rangle$ are, respectively,

$$\Delta_1 \doteq (6/7)\langle r^2\rangle(B_2^0-B_2^2);\ \Delta_2 \doteq (6/7)\langle r^2\rangle(B_2^0+B_2^2). \quad (11)$$

These energies are typically of the order of 10^2 to 10^3 cm^{-1}. With the additional relationship

$$\langle 3z^2-r^2|L_x^2-L_y^2|x^2-y^2\rangle = 2\sqrt{3},$$

the corresponding separation between the d_γ levels is likewise obtained. However, in most cases, these levels are about 10^4 cm^{-1} higher than the d_ϵ levels. Thus, at ordinary temperatures they do not contribute to the EFG, and, for the present, will be neglected.

It will prove convenient to express the EFG components in units of $(4/7)\langle r^{-3}\rangle$, that is

$$F_q' \equiv q_{\rm val}/(4/7)\langle r^{-3}\rangle \text{ and } F_{\eta q}' \equiv \eta_{\rm val} q_{\rm val}/(4/7)\langle r^{-3}\rangle. \quad (12)$$

These expressions lead to a factor, F', defined by

$$F' \equiv q_{\rm val}[1+\tfrac{1}{3}\eta_{\rm val}^2]^{1/2}/(4/7)\langle r^{-3}\rangle = [(F_q')^2+\tfrac{1}{3}(F_{\eta q}')^2]^{1/2}. \quad (13)$$

For the purposes of this section one then obtains

$$F_q' = Z^{-1}[1-\tfrac{1}{2}e^{-\Delta_1/kT}-\tfrac{1}{2}e^{-\Delta_2/kT}]$$

and

$$F_{\eta q}' = Z^{-1}[\tfrac{3}{2}e^{-\Delta_1/kT}-\tfrac{3}{2}e^{-\Delta_2/kT}], \quad (14)$$

where

$$Z = 1+e^{-\Delta_1/kT}+e^{-\Delta_2/kT}$$

so that

$$F' = Z^{-1}[1+e^{-2\Delta_1/kT}+e^{-2\Delta_2/kT}-e^{-\Delta_1/kT} -e^{-\Delta_2/kT}-e^{-(\Delta_1+\Delta_2)/kT}]^{1/2}. \quad (15)$$

The function, F', accounts for the temperature dependence of the quadrupole splittings. It vanishes at high temperatures because the EFG components arising from each state cancel one another. On the other hand, it approaches unity at low temperatures if the ground state is orbitally nondegenerate. This is true because, if any one of the states alone is occupied, $q_{\rm val}[1+\frac{1}{3}\eta_{\rm val}^2]^{1/2} = (4/7)\langle r^{-3}\rangle$ and $F'=1$. If, however, the two lowest d_ϵ states have the same energy, then F' becomes $\frac{1}{2}$ at low temperatures. This is most easily seen if $\Delta_1=\Delta_2<0$. Thus, Table I shows that an equal mixture of $|xz\rangle$ and $|yz\rangle$ alone will give $q_{\rm val}=-(2/7)\langle r^{-3}\rangle$ and $q_{\rm val}\eta_{\rm val}=0$, so that $F'=\frac{1}{2}$. Of course, if all three d_ϵ states are degenerate, then F' vanishes at any temperature (cubic symmetry).

Although the function, F', may be used to obtain an estimate of the energy separations, Δ_1 and Δ_2,[5,12] the above treatment best serves as a qualitative guide to the EFG in various symmetries. It is desirable, however, to represent the data by the equation

$$\Delta E = \tfrac{1}{2}e^2qQ(1-R)(4/7)\langle r^{-3}\rangle F, \quad (16)$$

where F is a reduction factor characteristic of the temperature and compound. Clearly, F' does not yet meet this requirement, since it does not explain the spread in the low-temperature values of ΔE in Fig. 1. Moreover, it is quite unlikely that variations of the term, $(1-R)\langle r^{-3}\rangle$, adequately explain this spread.

III. EFFECT OF THE SPIN-ORBIT INTERACTION

The spin-orbit interaction is presumably the primary cause of the spread in the low-temperature quadrupole splittings. This interaction is

$$V_{s.o.} = -\lambda \mathbf{L}\cdot\mathbf{S}, \quad (17)$$

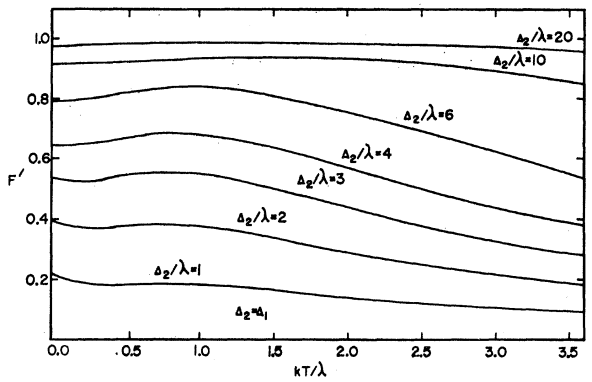

FIG. 3. Computer results for the reduction factor, F', plotted as a function of kT/λ for the axial case, $\Delta_1=\Delta_2$.

where the spin-orbit coupling constant, λ, is on the order of that for the free ion[16]: $\lambda_0=103$ cm^{-1}. By virtue of this interaction, the fivefold spin degeneracy of each orbital state is partially or completely lifted (Fig. 2) and its orbital character altered. Letting ψ_i refer to one of the spatial wave functions in Table I, and χ_j to one of the five spinors corresponding to $\mathbf{S}=2$, there will now be twenty-five ferrous wave functions of the form

$$\varphi_n=\sum_{i,j=1}^{5} A_{ij}{}^n\psi_i\chi_j, \tag{18}$$

whereas before they were of the simple form, $\psi_i\chi_j$. Thus one expects Eqs. (5) and (6) to lead to a reduction factor $F'(\Delta_1,\Delta_2,\lambda,T)$ still defined by Eq. (13) but different from Eq. (15).

The exact secular problem for the ferrous d_ϵ orbitals (diagonalization of a 15×15 matrix) has been worked out for the two axial cases, namely trigonal[14,17] and tetragonal.[18] For lower symmetries ($B_2{}^2\neq 0$) perturbation approximations may be used.[19] A perturbation approach of course depends upon the relative strengths of Δ_1, Δ_2, and λ, and therefore upon the compound. It is thus quite impractical, if not impossible, to give here any explicit formulas for the function, $F'(\Delta_1,\Delta_2,\lambda,T)$. This writer, however, has diagonalized via computer, many 15×15 and also 25×25 matrices[20] and obtained families of curves for a wide range of parameters, Δ_1/λ and Δ_2/λ and kT/λ. Therefore, here we limit ourselves to the qualitative features of the EFG calculation brought upon by including the spin-orbit interaction. These features will be illustrated by a few representative curves (Figs. 3–6) obtained from the computer calculations.

Qualitatively, the orbitally mixed states, φ_n, will yield smaller F' values then their pure counterparts, $\psi_i\chi_j$. As an example, consider how F', resulting from only one of the states, $|xy\rangle\chi_j$, behaves upon introduction of the spin-orbit interaction. Neglecting admixtures of the d_γ states this wave function becomes

$$\varphi=a|xy\rangle\chi_j+b|yz\rangle\chi_k+c|xz\rangle\chi_l, \tag{19}$$

where $a^2+b^2+c^2=1$ and $a^2\gg b^2$, c^2, and the χ's are any 3 orthogonal normalized spinors for which $\mathbf{S}=2$. Using Table I it is seen that for this state

$$F_q'=[a^2-(\tfrac{1}{2})b^2-(\tfrac{1}{2})c^2] \tag{20}$$

and

$$F_{\eta q}'=(\tfrac{3}{2})(b^2-c^2) \tag{21}$$

so that

$$F'=[\tfrac{3}{2}(a^4+b^4+c^4)-\tfrac{1}{2}]^{1/2}. \tag{22}$$

Since $a^4+b^4+c^4\leqslant 1$, it follows that F' is always smaller than unity, if b^2, $c^2\neq 0$. This argument is most appropriate at very low temperatures when only one state, φ_n, is occupied. Otherwise, one must, of course, first average the EFG components separately and then form the function F'. The reduction phenomenon still holds, however.

To understand the dependence of F' upon Δ_1, Δ_2 and λ, one may use perturbation theory to show

$$b\doteq M_1(\Delta_1/\lambda)^{-1} \quad \text{and} \quad c\doteq M_2(\Delta_2/\lambda)^{-1}, \tag{23}$$

where M_1 and M_2 are the appropriate matrix elements of $\mathbf{L}\cdot\mathbf{S}$. Thus, the smaller the ratios Δ_1/λ and Δ_2/λ, the more mixing and greater reduction. Exact (15×15) computer calculations[20] also show this to be true. In Figs. 3, 4, and 5, families of curves, F', are shown as functions of kT/λ for the cases, $\Delta_1=\Delta_2$, $\Delta_1=(\frac{1}{2})\Delta_2$, and $\Delta_1=0$, respectively. As in Sec. II, F' is reduced by approximately a factor of two when the lowest two orbitals are degenerate ($\Delta_1=0$). In Fig. 6, curves of constant F' are plotted as a function of Δ_1/λ and Δ_2/λ for a given

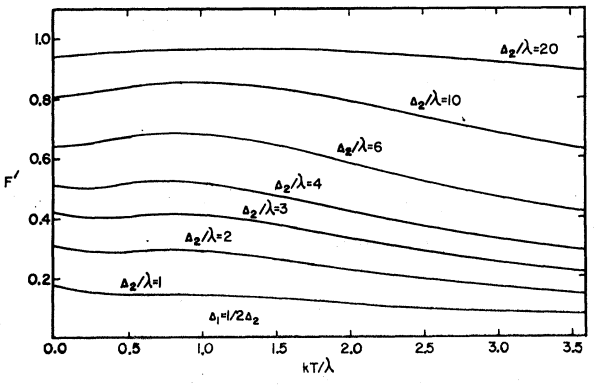

FIG. 4. Computer results for the reduction factor, F', plotted as a function of kT/λ for the case, $\Delta_1=\frac{1}{2}\Delta_2$.

[16] R. E. Trees, Phys. Rev. 82, 683 (1951).
[17] D. Palumbo, Nuovo Cimento 8, 271 (1958).
[18] A. Bose, A. S. Chakravarty, and R. Chatterjee, Proc. Roy. Soc. (London) A261, 207 (1961).
[19] K. Niira and T. Oguchi, Progr. Theoret. Phys. (Kyoto) 11, 425 (1954).
[20] R. Ingalls, Bull. Am. Phys. Soc. 8, 42 (1963). A detailed analysis of the quadrupole splitting and paramagnetic susceptibility in $Fe(NH_4SO_4)_2\cdot 6H_2O$ is in preparation.

"temperature" kT/λ. This figure illustrates how F' is lowered if either Δ_1/λ or Δ_2/λ is reduced. It also exhibits symmetry about the line, $\Delta_1=\Delta_2$, because the three d_ϵ states $|xy\rangle$ $|yz\rangle$ and $|xz\rangle$ are similar to each other, except for a choice of axes, and the spin-orbit interaction is isotropic. (If we had defined Δ_2 to be the over-all d_ϵ splitting, then one would also observe symmetry about the line $\Delta_1=0$, etc.) Consideration of the d_γ admixtures would only slightly alter ($\sim 1\%$) the quantitative results.

One final feature in Figs. 3 and 4 is the low-temperature decrease in the functions, F'. This is also best explained using perturbation theory. Since the orbital angular momentum for each state ψ_i is quenched ($\langle \mathbf{L} \rangle = 0$), one must go to second order to get the energy shifts brought upon by the spin-orbit interaction. If $|xy\rangle$ were the lowest orbital, then the second-order energy shift correspondingly to Eq. (19) would be

$$\Delta\epsilon \doteq -M_1^2\lambda^2/\Delta_1 - M_2^2\lambda^2/\Delta_2. \tag{24}$$

Thus all five $|xy\rangle\chi_j$ spin states would be lowered in energy, the lowest having the largest matrix elements, M_1 and M_2. But from Eqs. (22) and (23), this lowest spin state would also have the greatest admixture of the orbitals, $|yz\rangle$ and $|xz\rangle$, and therefore give the smallest EFG. This effect should manifest itself as a slight decrease in the quadrupole splitting at very low temperatures, in compounds for which Δ_1/λ and Δ_2/λ are on the order of 5. Some of the experimental results in Fig. 1 suggest this effect (for example, FeF_2, $Fe(NH_4SO_4)_2\cdot 6H_2O$, and $FeC_2O_4\cdot 2H_2O$), but, to this writer's knowledge, it has not been positively detected.

IV. SECONDARY EFFECT OF THE CRYSTALLINE FIELD

It remains to study the lattice EFG components, q_{lat} and $\eta_{\text{lat}}q_{\text{lat}}$. In principle, one may achieve some success by assuming the neighboring ions to be point charges and performing lattice summations,[21–23] for each compound, which are of the form

$$q_{\text{lat}} = \sum_i Z_i(3z_i^2 - r_i^2/r_i^5)$$

and

$$\eta_{\text{lat}}q_{\text{lat}} = \sum Z_i(3x_i^2 - 3y_i^2/r_i^5). \tag{25}$$

For our purposes, however, we may estimate these components by noticing that they are directly related to B_2^0 and B_2^2, and therefore also to Δ_1 and Δ_2. This is because $V_{\text{axial}}+V_{\text{rhombic}}$ is actually a quadrupole interaction between the ferrous ion and the lattice, which is of the same form as Eq. (1).

$$V_{\text{axial}}+V_{\text{rhombic}} \doteq \frac{e^2Q_{\text{val}}}{4L(2L-1)}\{q_{\text{lat}}[3L_z^2 - L(L+1)] + \eta_{\text{lat}}q_{\text{lat}}(L_x^2 - L_y^2)\}, \tag{26}$$

where

$$Q_{\text{val}} \equiv -\langle L=2, M_L=2 | 3z^2 - r^2 | L=2, M_L=2\rangle.$$

Upon comparison with Eqs. (10) one obtains

$$q_{\text{lat}} \doteq -4B_2^0/e^2 \doteq -(7/3)(\Delta_1+\Delta_2)/e^2\langle r^2\rangle \tag{27}$$

and

$$\eta_{\text{lat}}q_{\text{lat}} \doteq -12B_2^2/e^2 \doteq -7(\Delta_2-\Delta_1)/e^2\langle r^2\rangle. \tag{28}$$

These expressions are not strictly correct because: (i) Penetration of the ferrous ion by its crystalline neighbors is neglected in Eq. (26); (ii) a Sternheimer

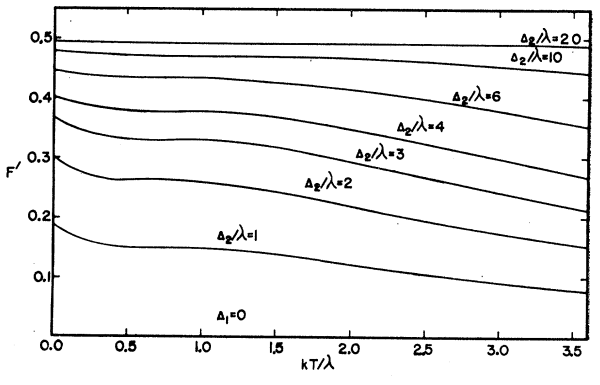

FIG. 5. Computer results for the reduction factor, F', plotted as a function of kT/λ for the axial case, $\Delta_1=0$.

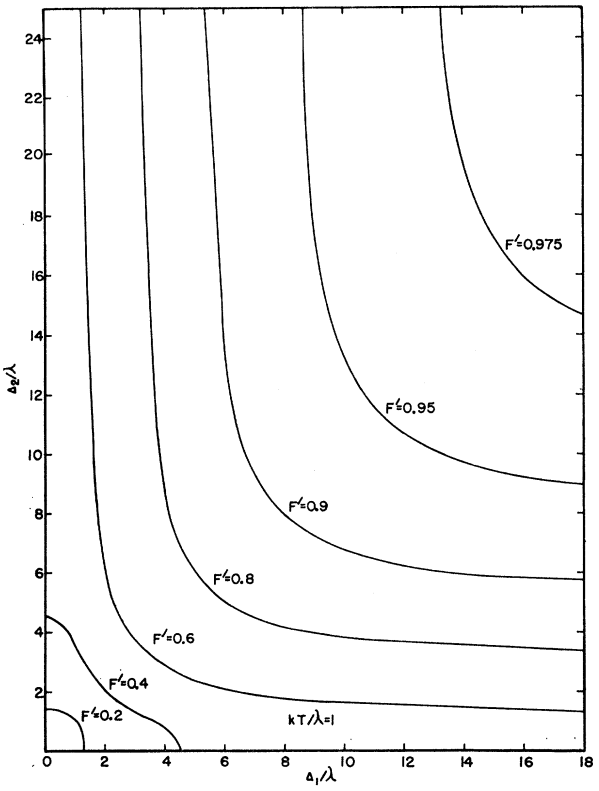

FIG. 6. Computer results for the reduction factor, F', plotted as a function of Δ_1/λ and Δ_2/λ for the case, $kT/\lambda=1$.

[21] R. Bersohn, J. Chem. Phys. **29**, 326 (1958).
[22] F. W. deWette, Phys. Rev. **123**, 103 (1961).
[23] G. Burns, Phys. Rev. **124**, 524 (1961).

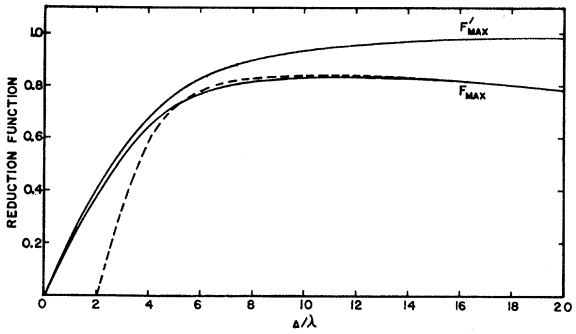

FIG. 7. Maxima of the reduction factors, F' and F, for the axial case, $\Delta_2=\Delta_1=\Delta$. The dashed line represents the limiting expression, $1-6(\Delta/\lambda)^{-2}-10^{-2}(\Delta/\lambda)$.

factor, $(1-\gamma)$, which would probably be somewhat greater than unity, is also neglected in Eq. (26); (iii) fourth-order axial and rhombic terms generally reduce somewhat the contribution of the second-order terms, B_2^0 and B_2^2, to Δ_1 and Δ_2. These errors partially cancel each other since (i) and (iii) cause underestimation of q_{lat} and $\eta_{\text{lat}}q_{\text{lat}}$, while (ii) causes overestimation. Moreover, since the lattice EFG is of only secondary importance to the quadrupole splitting, we shall neglect these errors.

It is now possible to estimate the desired function, $F=F(\Delta_1,\Delta_2,\lambda,T)$ appearing in Eq. (16). This function may be defined implicitly in a manner similar to Eq. (13).

$$F=[F_q^2+(\tfrac{1}{3})F_{\eta q}^2]^{1/2}, \tag{29}$$

where, using Eqs. (3), (4), (12), (27), and (28)

$$F_q\equiv\frac{q}{(1-R)(4/7)\langle r^{-3}\rangle}$$

$$=F_q'-\frac{49}{12}\frac{(1-\gamma_\infty)}{(1-R)}\frac{(\Delta_1+\Delta_2)}{e^2\langle r^{-3}\rangle\langle r^2\rangle}, \tag{30}$$

and

$$F_{\eta q}\equiv\frac{\eta q}{(1-R)(4/7)\langle r^{-3}\rangle}$$

$$=F_{\eta q}'-\frac{49}{4}\frac{(1-\gamma_\infty)}{(1-R)}\frac{(\Delta_2-\Delta_1)}{e^2\langle r^{-3}\rangle\langle r^2\rangle}. \tag{31}$$

The most important point here is that the lattice EFG components are always of opposite sign to those from the valence charge distribution and therefore reduce the effects of the latter upon the quadrupole splitting. It is also noteworthy that this reduction effect increases with Δ_1 and Δ_2, whereas the spin-orbit reduction of the last section decreases with these parameters. One may obtain an understanding of the relation between these competing effects by assuming

$$\Delta_1=\Delta_2=\Delta\gg\lambda \quad\text{and}\quad \lambda\ll kT\ll\Delta. \tag{32}$$

This gives us the case where the lowest five states, of the form in Eq. (19), are alone occupied and also equally populated. Therefore F' should be at its maximum. It is then straightforward to use perturbation theory and average the five resulting expressions of the form in Eq. (20) to obtain

$$F_{\max}'\doteq 1-6(\Delta/\lambda)^{-2}. \tag{33}$$

To calculate the lattice contribution in Eq. (30), one may use the following free-ion estimates[16,7,8]:

$$\begin{aligned}\lambda&\doteq\lambda_0=10^2\ \text{cm}^{-1},\\ \langle r^2\rangle&\doteq\langle r^2\rangle_0=1.4\ \text{a.u.},\\ (1-R)\langle r^{-3}\rangle&\doteq(1-R_0)\langle r^{-3}\rangle_0=3.3\ \text{a.u.},\\ (1-\gamma_\infty)&\doteq(1-\gamma_{\infty_0})\doteq 12,\end{aligned} \tag{34}$$

obtaining

$$\frac{49}{6}\frac{(1-\gamma_\infty)}{(1-R)}\frac{\lambda}{\langle r^{-3}\rangle\langle r^2\rangle e^2}\doteq 10^{-2}. \tag{35}$$

This then yields the reduction function

$$F_{\max}\doteq 1-6(\Delta/\lambda)^{-2}-10^{-2}(\Delta/\lambda). \tag{36}$$

This approximate expression is shown in Fig. 7, together with the "exact" curve, obtained by subtracting 10^{-2} (Δ/λ) from the maxima of the curves in Fig. 3. The

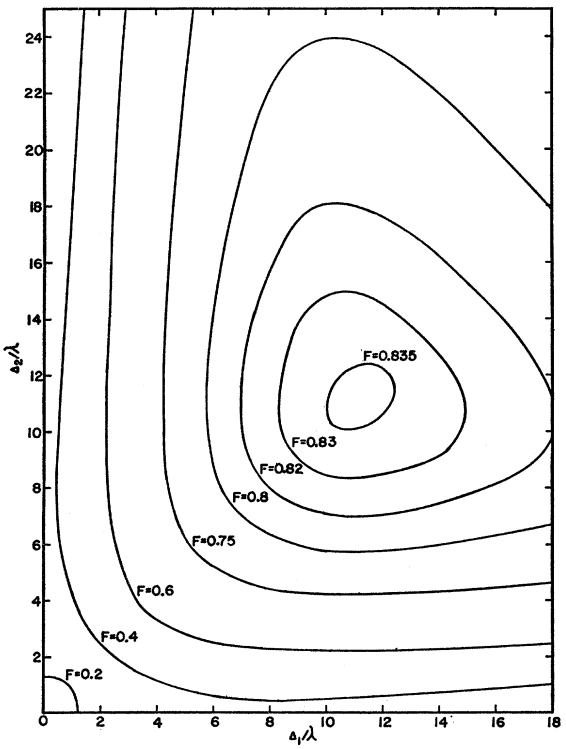

FIG. 8. Maxima of the reduction function, F, plotted as a function of Δ_1/λ and Δ_2/λ.

family of curves, $F_{\max}(\Delta_1/\lambda,\Delta_2/\lambda)=$const., which include the secondary crystalline field EFG corrections, is shown in Fig. 8. It is seen that $F_{\max}$ reaches its largest value of 0.83 near the region, $\Delta/\lambda=11$. Therefore, in the solid, one generally expects q to be reduced from $(4/2)(1-R)\langle r^{-3}\rangle$ by *at least* 17%. From the above, it may be remarked that, were it not for the large Sternheimer effect, the lattice EFG contribution would be completely negligible.

As a side effect, it is noted that there should be some temperature at which F goes to zero because the EFG from the valence electron is small enough to exactly cancel that from the lattice. Above this temperature the quadrupole interaction will change sign. This behavior has been observed in[24] Tm^{169}, and is made possible because of the large Sternheimer enhancement,[25] $1-\gamma_\infty$. In ferrous compounds, however, one may have trouble because of discouraging effects such as chemical changes and low recoilless absorption.

V. COVALENCY EFFECTS

In the foregoing treatment, symmetry considerations have been used to modify the spin and orbital parts of the free-ion $3d$ wave functions. There remains the problem of changes in the radial parts of these wave functions, due to the lattice, and the resulting change in $\langle r^{-3}\rangle$, $\langle r^2\rangle$, λ, R and γ_∞. Owen[26] has observed that the effective spin-orbit coupling constant is somewhat smaller in the crystal than in the free ion. He and others[27–29] have used the method of molecular orbitals[30] to show that λ and λ_0 are related by

$$\lambda=\alpha^2\lambda_0, \tag{37}$$

where the "covalency factor," α^2, is generally between 0.6 and 0.9. Marshall and Stuart[31] have suggested that radial expansion due to screening is the main cause of the reduction, and their suggestion has in turn been questioned by Shulman and Sugano.[29] Regardless of the cause, however, it is generally agreed that there is a fractional decrease in λ and the same fractional decrease in the effective value of $\langle r^{-3}\rangle$, since the two are roughly proportional to one another. Since the corresponding changes in $\langle r^2\rangle$, R, and γ_∞ are not known, and probably not so important for our purposes, we are forced to ignore them.

It must then suffice here to observe what happens when covalency factors are introduced into the results of the last three sections. Least important will be the change in the small crystalline EFG terms in Eq. (30) and Eq. (31), since, for example, both the numerator and the denominator in Eq. (35) are reduced. Of more importance is the fact that F' (or F) is a function of Δ_1/λ, Δ_2/λ and kT/λ, so that the reduction of the free-ion spin-orbit coupling constant, in effect, reduces the free-ion energy and temperature scales by the factor, α^2. Of most importance, however, is the term $\langle r^{-3}\rangle$ in Eq. (16), since it governs the magnitude of the quadrupole splitting. Therefore, if the free-ion value of $\langle r^{-3}\rangle_0$ is used, it is also reasonable to multiply it by α^2. Thus, one may write

$$\Delta E\doteq(2/7)e^2Q(1-R_0)\langle r^{-3}\rangle_0\alpha^2F(\Delta_1,\Delta_2,\alpha^2\lambda_0,T). \tag{38}$$

Presumably, variations in α^2 account somewhat for the differences in the low-temperature quadrupole splittings.

VI. CALCULATION OF Q FROM $FeSiF_6\cdot6H_2O$ DATA

With expression Eq. (38) in mind it is worthwhile summarizing the various estimates of Q from ferrous quadrupole splitting data. Neglecting the factors, $1-R_0$, α^2, and F, and using[9] $\langle r^{-3}\rangle_0=5.1$ a.u., calculated from Watson's[32] restricted Hartree-Fock wave functions, one obtains Q values ranging from 0.09b to 0.12b, depending upon the compound.[2,4,9] The value of 0.12b was obtained from the trigonal compound, $FeSiF_6\cdot6H_2O$. The EFG in this compound was presumably least affected by spin-orbit coupling, since Palumbo,[17] in an analysis of the paramagnetic susceptibility data, had estimated the axial splitting to be, $\Delta=1200$ cm^{-1}. (Figure 7 shows that the spin-orbit effect would only reduce the EFG by 3 or 4%.) Subsequently, a variational calculation of the Sternheimer factor,[7] $R_0=+0.22$, brought this estimate of Q up to 0.15b. Recent unrestricted Hartree-Fock calculations[8] have yielded $(1-R_0)\langle r^{-3}\rangle_0=3.3$ a.u. ($R_0=+0.32$ and $\langle r^{-3}\rangle_0=4.8$ a.u.), thus increasing Q to 0.18b. The paramagnetic susceptibility and quadrupole data for $FeSiF_6\cdot6H_2O$ have also been analyzed by Eicher,[14] who, neglecting core polarization, and the crystalline EFG, but correcting for spin-orbit effects, estimates $\Delta/\lambda=7.5$ and $Q=0.15$b. As with Palumbo, Eicher's determination of Δ/λ is not altogether satisfactory, probably because of variation of Δ with temperature, covalency, and crystalline fields of lower symmetry.

It remains here to take into account the effects of the crystalline EFG and covalency in explaining the quadrupole data of $FeSiF_6\cdot6H_2O$. Although Eicher's value of $\Delta/\lambda=7.5$ seems a bit low, (Sec. VII) one is fortunate in that $F_{\max}$ (see Fig. 7) is relatively insensitive to Δ/λ in the range, 8 to 15. In this region, $F_{\max}=0.83$ which one may assume corresponds to the

[24] R. Cohen, U. Hauser, and R. L. Mössbauer, in *The Mössbauer Effect*, edited by D. M. J. Compton and A. A. Schoen (John Wiley & Sons, Inc., New York, 1962); R. Cohen (private communication).
[25] R. E. Watson and A. J. Freeman, Bull. Am. Phys. Soc. **8**, 24 (1963).
[26] J. Owen, Proc. Roy. Soc. (London) **A227**, 183 (1955).
[27] M. Tinkham, Proc. Roy. Soc. (London) **A236**, 549 (1956).
[28] W. Low, *Paramagnetic Resonance in Solids* (Academic Press Inc., New York, 1960).
[29] R. G. Shulman and S. Sugano, Phys. Rev. **130**, 506 (1963), and S. Sugano and R. G. Shulman, Phys. Rev. **130**, 517 (1963).
[30] J. H. Van Vleck, J. Chem. Phys. **3**, 807 (1935).
[31] W. Marshall and R. Stuart, Phys. Rev. **123**, 2048 (1961).
[32] R. E. Watson, Technical Report No. 12, Solid State and Molecular Theory Group, Massachusetts Institute of Technology, 1959 (unpublished).

TABLE II. Parameters used in describing the Fe^{57m} quadrupole splitting observed in several ferrous compounds. The theoretical curves, obtained using these parameters, are compared with the experimental data in Fig. 1.

Compound	α^2	Δ_1 (cm^{-1})	Δ_2 (cm^{-1})	Ground-state orbital wave function
$FeSiF_6 \cdot 6H_2O$	0.80	760	760	$\|3z^2-r^2\rangle$
$FeSO_4 \cdot 7H_2O$	0.80	480	1300	$\|xy\rangle$
$Fe(NH_4SO_4)_2 \cdot 6H_2O$	0.80	240	320	$\|xy\rangle$
$FeC_2O_4 \cdot 2H_2O$	0.80	100	960	$\|xy\rangle$
$FeSO_4$	0.80	360	1680	$\|x^2-y^2\rangle+0.09\|3z^2-r^2\rangle$
$FeCl_2 \cdot 4H_2O$	0.80	750	2900	$\|x^2-y^2\rangle+0.10\|3z^2-r^2\rangle$
FeF_2	0.67	1000	2200	$\|x^2-y^2\rangle+0.14\|3z^2-r^2\rangle$

maximum, low-temperature, quadrupole splitting,[4] $\Delta E=0.37$ cm/sec. With these results and the unrestricted Hartree-Fock value for $(1-R_0)\langle r^{-3}\rangle_0$, one obtains

$$\alpha_f^2(2/7)e^2Q(1-R_0)\langle r^{-3}\rangle_0 \doteq (0.37 \text{ cm/sec})/0.83 \doteq 0.45 \text{ cm/sec} \quad (39)$$

and

$$\alpha_f^2 Q \doteq 0.23\text{b}, \quad (40)$$

where α_f^2 is the covalency factor for $FeSiF_6 \cdot 6H_2O$. Making the reasonable estimate[26,28,33]:

$$\alpha_f^2 \doteq 0.80 \pm 0.05,$$

one obtains

$$Q \doteq (0.29 \pm 0.02)\text{b}. \quad (41)$$

It is seen that the combined effects of the crystalline field, spin-orbit interaction, core polarization and covalency can reduce the EFG from the unpolarized, free-ion value by more than a factor of two.

It is noteworthy that a recent recalculation of the ferric Sternheimer factor,[34] γ_∞, has led one to the value, $Q=0.28$b, from ferric Mössbauer data[35,36] and calculations of the pertinent lattice summations.[23]

VII. BRIEF SURVEY OF THE FERROUS QUADRUPOLE SPLITTING DATA

Possibly the most useful result of the foregoing analysis is that the ferrous quadrupole splittings may be written as [from Eq. (39)]

$$\Delta E(\text{cm/sec}) \doteq 0.45(\alpha^2/\alpha_f^2)F(\Delta_1, \Delta_2, \alpha^2\lambda_0, T). \quad (42)$$

Thus, uncertainties in Q, R, and $\langle r^{-3}\rangle$, are, in a sense, bypassed, and the splittings expressed as a function of three adjustable parameters, Δ_1, Δ_2, α^2. In principle, one may then assume a value for α^2 (and λ), and, for each temperature, plot the curves, $F=F_{\text{exp}}=\text{const}$, as a function of Δ_1/λ and Δ_2/λ, in a manner similar to Fig. 8. If the energy level scheme in Fig. 2 holds and Δ_1 and Δ_2 do not vary with temperature, the F curves for all temperatures will roughly intersect at a point, enabling one to determine both Δ_1 and Δ_2. In this way, one obtains the parameters listed in Table II, and the corresponding solid curves of Fig. 1, which agree reasonably well with experiment.

For $FeSiF_6 \cdot 6H_2O$, with the choice of $\alpha^2=0.8$, one necessarily uses the ratio, $\Delta/\lambda=9.5$, to obtain the measured high-temperature decrease in quadrupole splitting.[4] Eicher[14] uses the values $\Delta/\lambda=7.5$ and $\alpha^2=1$, to obtain the same decrease. For $FeSO_4 \cdot 7H_2O$, $FeC_2O_4 \cdot 2H_2O$ and $Fe(NH_4SO_4)_2 \cdot 6H_2O$ fair agreement with experiment is also obtained with the choice, $\alpha^2=0.8$. A more detailed analysis of this last compound[20], however, indicates that the crystal-field splittings, Δ_1 and Δ_2, are quite temperature-dependent, presumably because of anisotropic thermal expansion.

For the compounds, $FeSO_4$, $FeCl_2 \cdot 4H_2O$ and FeF_2, no agreement with experiment is obtained until one assumes the rhombic distortion to be of such a nature that the ground-state orbital is of the form[37,9] $|x^2-y^2\rangle + \delta|3z^2-r^2\rangle$, rather than $|xy\rangle$. Thus, for these compounds, to preserve the form of the rhombic crystalline field term of Eq. (7), the x and y axes are rotated about the z direction by 45°. This rotation in turn interchanges the states $|xy\rangle$ and $|x^2-y^2\rangle$, the latter being coupled to $|3z^2-r^2\rangle$ by the rhombic field, (Sec. II). Indeed, one may use perturbation theory and the results of Sec. II to show

$$\delta \doteq \frac{\sqrt{3}(\Delta_2-\Delta_1)}{3[E(d_\gamma)-E(d_\epsilon)]+2(\Delta_1+\Delta_2)}. \quad (43)$$

In this manner, one estimates the energy difference, $E(d_\gamma)-E(d_\epsilon)$, to be approximately 7800, 9600, and 3200 cm^{-1}, for $FeSO_4$, $FeCl_2 \cdot 4H_2O$, and FeF_2, respectively. For the compound, FeF_2, the covalency factor was chosen to agree with Tinkham's[27] estimate, ($\alpha^2 \doteq 0.6 \pm 0.1$). The parameters, Δ_1, Δ_2, and α^2, for this compound, yield the asymmetry parameter, ($\eta=0.33$), measured by Wertheim[1], and the approximate d_ϵ energy splittings proposed by Moriya *et al.*[37] Apparently strong covalency and second-order crystalline fields account for the small quadrupole splitting in this compound and its remarkable lack of dependence upon temperature.

It must be noted here that the parameters listed in Table II are not unique, since, with the exception of the cases of $FeSiF_6 \cdot 6H_2O$ and FeF_2, they were chosen to fit the Mössbauer data, alone, over a wide temperature range. An obvious improvement, of course, would be to simultaneously analyze, at many temperatures, quadrupole splittings, paramagnetic susceptibilities and specific heats, as well as resonance data (if they exist).

[33] C. E. Johnson (private communication).
[34] R. M. Sternheimer, Phys. Rev. **130**, 1423 (1963).
[35] C. Alff and G. K. Wertheim, Phys. Rev. **122**, 1414 (1961).
[36] D. N. E. Buchanan and G. K. Wertheim, in *The Mössbauer Effect*, edited by C. M. J. Compton and A. A. Schoen (John Wiley & Sons, Inc., New York, 1962), p. 130.
[37] T. Moriya, K. Motzuki, J. Kanamori, and T. Nagamiya, J. Phys. Soc. Japan **11**, 211 (1956).

VIII. SUMMARY

In this work, one has endeavored to express the EFG tensor in ferrous compounds in terms of the d_ϵ splitting parameters, Δ_1 and Δ_2, and also the covalency factor, α^2, which roughly governs the values of $\langle r^{-3}\rangle$ and the spin-orbit coupling constant, λ. In doing so, detailed study of the complete problem, ferrous ion plus ligands, has necessarily been avoided. At the same time one has gained some insight as to the actual behavior of the complete EFG tensor, as a function of axial and rhombic field strengths, and, of course, temperature.

This study has also permitted one to make an estimate of the electric quadruploe moment of Fe^{57m} which essentially agrees with that obtained from studies of ferric compounds. At the same time, the Mössbauer data alone permits one to estimate crystalline field splittings which are generally consistent with those obtained from other methods. Therefore, the electric quadrupole splittings measured by the Mössbauer method should prove to be a valuable aid in understanding, not only ferrous compounds, but other paramagnetic substances, as well.

ACKNOWLEDGMENTS

The author is grateful to S. DeBenedetti, S. A. Friedberg, C. E. Johnson, and R. Cohen for stimulating talks; to R. E. Watson and A. J. Freeman for a preprint of their paper; to K. Kumar for the use of his matrix-diagonalization computer program; and to P. Zory for preliminary low-temperature Mössbauer results.

PHYSICAL REVIEW VOLUME 133, NUMBER 3A 3 FEBRUARY 1964

Effect of a Static Electric Field on the R Lines of $(3d)^3$ Ions in Corundum

M. D. STURGE
Bell Telephone Laboratories, Murray Hill, New Jersey
(Received 6 September 1963)

The pseudo-Stark splitting of the R lines of V^{2+} and Mn^{4+} in Al_2O_3 has been measured in electric fields up to 170 kV/cm. For fields parallel to the c axis the splitting is 1.5×10^{-6} cm^{-1}/(V/cm) for V^{2+} and 4.5×10^{-5} for Mn^{4+} (compare 5.3×10^{-6} for Cr^{3+}). There is no detectable splitting for an electric field perpendicular to the c axis. The effect for Mn^{4+} is much greater than one would expect from the oscillator strengths of the crystal-field transitions, which, like the pseudo-Stark splitting, depend primarily on the hemihedral part of the crystal field. The large effect in Mn^{4+} appears to be principally due to the movement of the ion in the field and the consequent change in overlap with its neighbors. The principal effect for the other two ions appears to be polarization of the ion itself.

INTRODUCTION

CONSIDER an impurity ion in a substitutional position in an otherwise perfect lattice. If the ion is at a center of symmetry, its electronic wave functions have a definite parity. In this case an odd parity perturbation, such as that due to an applied electric field, has no diagonal matrix elements, and can produce no first-order effect on the energy levels. This is a well-known result in atomic spectroscopy, where a linear Stark effect is only observed in the case of hydrogen, in which levels of odd and even parity are "accidentally" degenerate. If the ion is not at a center of symmetry, on the other hand, parity is no longer a good quantum number, and a shift of the energy level linear in electric field can, in principle, occur. It is usually sufficiently accurate to treat the deviation from inversion symmetry as a small perturbation mixing levels of well defined parity.

The corundum ($\alpha-Al_2O_3$) lattice has D_{3d} symmetry, but an individual Al^{3+} ion is not at a center of symmetry and its site has only C_3 symmetry (see Fig. 1) sites of type a and b being connected by inversion through the point d. An electric field applied along the c axis acts in equal and opposite senses on ions at the two sites, shifting their energy levels in opposite directions. Thus, an apparent splitting of a level can be produced, called by Kaiser, Sugano, and Wood[1] (who first observed the effect optically) the pseudo-Stark splitting. This paper reports an extension of their measurements on ruby (chromium-doped corundum) to the isoelectronic ions V^{2+} and Mn^{4+} in the same lattice. The size of the splitting varies by a factor of 30 through the isoelectronic sequence, although the optical spectra are in other respects very similar. Comparison of the results with simple models shows that we have to take into account the change in covalency produced by the motion of the ion in the electric field in order to explain them.

EXPERIMENTAL

Specimens of corundum containing V^{2+} (concentration of the order one part in 10^5) were prepared by

[1] W. Kaiser, S. Sugano, and D. L. Wood, Phys. Rev. Letters 6, 605 (1961).